Finite element simulation study on influence of spacecraft stiffener structure on elastic wave propagation

Xu Bian[1] , *Biwan* Tian[1,*], and *Shijiu* Jin[2]

[1]Tianjin University Renai College, Tianjin, China
[2]State Key Laboratory of Precision Measurement Technology and Instrument, Tianjin University, Tianjin, China

Abstract. Aiming at the propagation process of elastic wave in spacecraft stiffener structure. In this paper, the phase and energy changes of elastic waves propagating in the wall structure of stiffeners at different frequencies are analyzed by using finite element method and laser Doppler vibrometer (LDVS). Meanwhile, the relationship between the parameters of stiffeners and the diffusion of acoustic wave energy and the phase change of elastic waves respectively is obtained. The results show that in the range of parameters involved in this paper, the stiffener has a significant effect on elastic waves propagation. When wavelength $\lambda >$ 10mm, most of the elastic waves are reflected by the stiffener, while when $\lambda <$ 6mm, elastic waves propagate more easily across the stiffener, and the proportion of those propagated by the stiffener increases. Moreover, the functional expression of the relationship between the height of the stiffener and the frequency of the elastic wave which can easily propagate through the stiffener is obtained.

1 Introduction

Recently, with the development of manned space flight the real time detection and locating technology for spacecraft leakage becomes the focus of research as protecting astronaut life safety. With many advantages, locating method based on detecting the elastic waves existed by leakage source in wall is becoming an important research direction. However due to the complexity of spacecraft wall structure, it makes detection and locating results worse in actual situations. Therefore, to solve this problem, we need to study deeply the influence of spacecraft wall structure on leakage excited elastic wave propagation. Based on the previous research [1], aiming at the influence of stiffener structure on spacecraft wall, starting from its influence on propagating distance and stability of elastic wave, this paper studies the relation between height/width parameters and elastic wave propagation phase and energy by establishing finite element simulation model. Moreover, combined with laser Doppler vibration measurement results, more accurate and abundant

* Corresponding author: bx332@tju.edu.cn

data are obtained as well. On one hand, data support is provided for locating algorithm based on elastic wave. On the other hand, it provides reference for spacecraft wall design.

Many scholars have studied propagation characteristics of acoustic in the wall with finite element simulation method and obtained many significant results. P.E. Lhuillier et al [2] have simulated propagation of ultrasonic wave in various anisotropic weld materials by finite element method, and discussed the effect of scattering on ultrasonic attenuation in polycrystalline materials. Pettit J R [3] discussed the influence of rough defects on ultrasonic propagation using finite element method (FEM). S. A. Shcherbinin et al [4] have performed the finite-element simulations of standing cylindrical waves formation inside the cylindrical transducer filled with a liquid by those oscillation modes of piezoelectric cylinder using ANSYS software package and compared effectiveness of different regimes of standing waves generation. Christensen et al [5] analyzed the effects of viscosity and thermal conductivity on acoustic propagation in rigid tubes with different sections shapes using COMSOL software and compared with ACTRAN results. Taking the axial and circumferential defects with different sizes as research objects, Hu Hongwei et al [6] have studied the relationship between the defect location and defect size with the ultrasonic guided wave reflection coefficients, using a control variable method, by finite element simulation. Ai Chunan et al [7] simulated propagation problems of ultrasonic wave in fluid, isotropic materials and anisotropic materials and discussed feasibility of finite element method applied to ultrasonic propagation simulation. Fu Xibin [8] analyzed ultrasonic response characteristics of welded joint of pressure vessel by finite element analysis and analyzed different probe parameters such as center distance frequency angle etc. influence on detection result. Ye Hanfeng et al [9] established oblique incident simulation model of acoustic overlay element of double layer cavity using finite element software COMSOL and studies the influence of overlay structure and material parameters on sound absorption performance under oblique incidence condition.

In fact, considering weight, the thickness of wall with structure is usually less than 10 mm. According to theoretical derivation [1], elastic wave excited by leakage source mainly propagates in lamb form under this condition which will be affected by the stiffener structure on the wall obviously. This paper uses finite element simulation and Laser Doppler vibration measurement method to research and discuss influence of different size stiffener structures on elastic wave propagation and obtain corresponding conclusions.

2 Research methods

Within a period of time, the signal excited by leakage source satisfies the Dirichlet condition, and can be expanded as shown in equation 1:

$$P(t) = A_0 + \sum_{n=1}^{\infty} A_n \sin(n\omega t + \phi_n) \tag{1}$$

In other words, research objectives can be decomposed into several elastic waves with different frequency. Therefore, in this paper, the energy attenuation and phase distortion of elastic waves with different frequencies have been studied in order to clarify the influence of stiffener structure on elastic wave propagation. According to the frequency distribution characteristics of elastic waves excited by the leakage source in the wall [1], the research frequency band is selected as $f \in [20,400]$ kHz. Combined with the periodicity and symmetry of the excitation signal in the spatial distribution, two points P and Q are set in the model to excite and collect the elastic wave S(t) respectively. In order to ensure the consistency of the research conditions, the structure without stiffener is used as the background experimental data. That is to say, when there is a stiffener structure, the normal

displacement data of the wall collected by Q-point is $S_Q(t)$, while when there is no stiffener structure, the Q-point acquisition signal is $S_Q'(t)$. Then, in the time range $[t_1, t_2]$, the effect of stiffener on the phase of elastic waves can be defined by cross-correlation, as shown in equation 2.

$$R_{QQ'}(\tau) = \int_{t=t_1}^{t_2} S_Q(t) \cdot S_{Q'}(t+\tau) dt \tag{2}$$

At the same time, in two cases, consider the signal energy received by Q point in the time range $[t_1, t_2]$, the energy dissipation ratio can be defined as:

$$\alpha_{QQ'} = \frac{\int_{t=t_1}^{t_2} \left|S_Q(t)\right|^2 dt}{\int_{t=t_1}^{t_2} \left|S_{Q'}(t)\right|^2 d} \tag{3}$$

2.1 Finite element simulation

In order to get the data of P point and Q point, a model of stiffener wall has been established in this paper which the length, width and height are $100 \times 50 \times 2.5$mm respectively, and $d \in [1,6]$mm, $h \in [1,31]$mm as the thickness and height of the stiffener base on the actual situation of the spacecraft wall and computing scale. The perfectly matched layer is used to eliminate the influence of the edge of the model on the elastic wave propagation in order to simulate the infinite region, and the thickness of each matching layer is determined as 10mm according to the analyzed elastic wave frequency. Meanwhile, the magnesium-aluminium alloy is selected as the material of the wall model. The model mainly uses the method of free tetrahedron division to meet the needs of computational efficiency and simulation accuracy. Meanwhile, according to the requirements of elastic wave sample in spatial domain, the maximum cell size of the mesh is set as less than 1/6 wavelengths. Combined with the calculation of dispersion curve, the maximum cell size of meshing in the range of frequency should be less than 1mm. The model and its meshing result are shown in Fig 1 (a). Meanwhile, taking the propagation of the f=300kHz ultrasonic wave excited from the P point in the stiffener (d=4mm, h=20mm) as an example, the transient simulation results of the particle z-axis vibration displacement (unit m) in t=0.04ms are shown in Fig 1 (b).

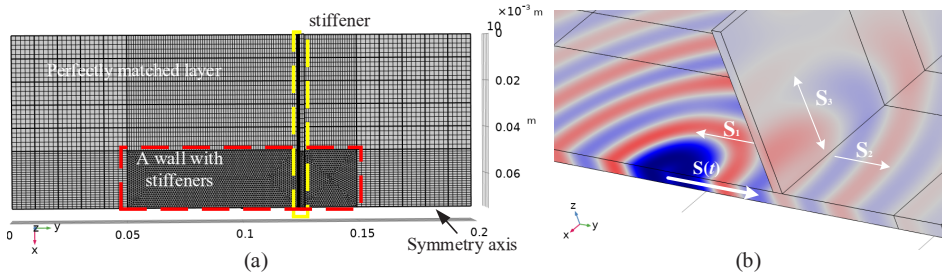

Fig. 1. Finite element simulation model and transient simulation in time domain (a. Finite element simulation model; b. transient simulation in time domain f=300kHz, t=0.04ms).

When the elastic wave propagates towards the stiffener structure, one part (S_3) enters the stiffener and continues to propagate, the other part (S_1) is reflected in the form of echo,

and only part of the elastic wave (S_2) can propagate directly through the stiffener. As a result, the elastic wave passes through the structure and produces obvious energy dissipation. Through the analysis of the simulation results, when there is a stiffener, the Q-point acquisition signal is mainly composed of two parts, one is the elastic wave propagating directly through the stiffener structure, and the other is the elastic wave coupled to the wall after propagating in the stiffener for a period of time. Let t_a represents the time required for the elastic wave to propagate from the P point to the Q point through the wall without stiffener, and t_b represents the propagation time of the elastic wave in the stiffener, γ represents the amplitude attenuation coefficient of the elastic wave passing through the stiffener, η represents the amplitude attenuation coefficient of the elastic waves propagated by stiffeners, then:

$$\begin{cases} S_{Q'}(t) = S(t_0 + t_a) \\ S_Q(t) = \gamma \cdot S(t_0 + t_a) + \eta \cdot S(t_0 + t_a + t_b) \end{cases} \tag{4}$$

Combined with the dispersion characteristics of elastic waves propagating in a thin plate, it is known that except ta is only related to *f*, other variables are related to *h*, *d* and *f*, that is, the different values of these three parameters have a significant impact on $R_{QQ'}$ and $\alpha_{QQ'}$.

2.2 Laser Doppler vibration measurement experiment

This phenomenon can also be measured directly by experiments, and laser doppler vibrometer (LDV) have been used to measure actual measurements so as to obtain more accurate and abundant experimental data. Some stiffener structure is selected and the propagation of elastic wave is measured by Polytec PSV- 500 laser doppler vibrometer. This vibrometer is an all-digital scanning laser vibrometer, which can be used for non-contact full-field measurement on the target, and the particle vibration can be obtained. Taking the *f*=200kHz ultrasonic signal as an example, the experimental results are shown in Fig 2.

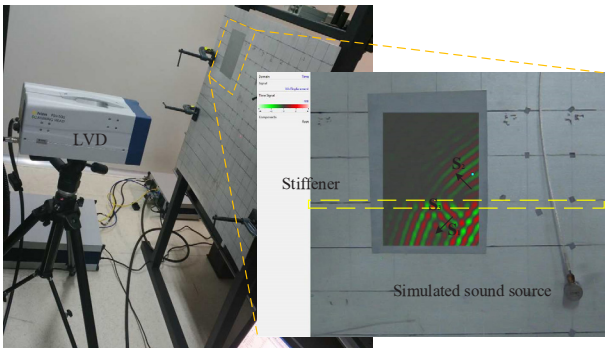

Fig. 2. The experimental platform of LDV Measurement and the results of an experiment.

The existences of S_1, S_2 and S_3 can also be clearly seen in Fig 2, which are consistent with those shown in Fig 1 (b). At the same time, according to the research and analysis of the data, more accurate and abundant data can be obtained.

3 Data analysis

Through the above two methods, the experimental data are calculated and sorted out. Two three-dimensional matrices $R_{QQ'}$ and $\alpha_{QQ'}$ about *d*, *h* and *f* are obtained, which are recorded as $\mathbf{R}^{k\times m\times n}(d,h,f)$ and $\boldsymbol{\alpha}^{k\times m\times n}(d,h,f)$. Where *k*, *m* and *n* represent the number of elements contained in the corresponding dimensions in the matrix, respectively. For the sake of discussion and expression, select *d*=2mm, 4mm, 6mm respectively, then the value distribution map **R**(*h*,*f*) and **α**(*h*,*f*) are shown in Fig 3.

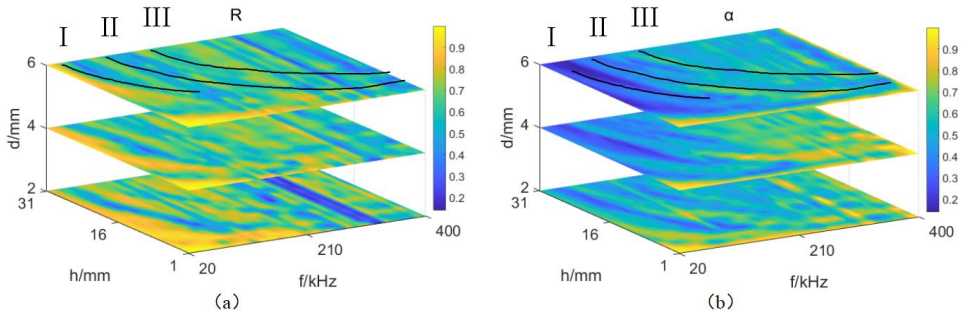

Fig. 3. Value distribution (a. $\mathbf{R}_{d=2,4,6}(h,f)$; b. $\boldsymbol{\alpha}_{d=2,4,6}(h,f)$).

As shown in Fig 3, on the whole, the distribution rules of $R_{QQ'}$ and $\alpha_{QQ'}$ are not consistent. Combined with equation (4), it shows that this phenomenon is mainly caused by the phase inconsistency between $\gamma\cdot S(t_0+t_a)$ and $\eta\cdot S(t_0+t_a+t_b)$. The existence of stiffeners will increase the propagation path of some elastic waves and form elastic waves with different phases at Q point. when they superpose on each other, they will have different effects on the phase and amplitude of $S_Q(t)$, and the degree of influence is closely related to the values of *d*, *h* and *f*, which leads to differences in the distribution of $R_{QQ'}$ and $\alpha_{QQ'}$.

3.1 Effect of stiffener thickness (*d*) on elastic wave propagation

According to Fig 3, compared with the thickness of stiffener, the effect of elastic wave frequency on $R_{QQ'}$ and $\alpha_{QQ'}$ is more significant. $R_{QQ'}$ and $\alpha_{QQ'}$ are comb-like distribution whose change trends are different. There are two points 180kHz and 300kHz in the frequency domain which divide the frequency domain into three regions. Combined with equation (4), the results of our analysis are as follows:

• when the elastic wave wavelength $\lambda > 10$mm ($f < 180$kHz), the mean value of $R_{QQ'}$ is smaller and increases with the increase of frequency. Most of the elastic wave are reflected by the stiffener, that is, the value of $S_Q(t)$ is mainly determined by $\gamma\cdot S(t_0+t_a)$.

• when the elastic wave wavelength $\lambda < 6$mm ($f > 300$kHz), the mean value of $R_{QQ'}$ is larger and increases with the increase of frequency. It is easier to propagate through the stiffener, moreover, the proportion of $\eta\cdot S(t_0+t_a+t_b)$ in $S_Q(t)$ increases, the influence on the phase of $S_Q(t)$ increases.

3.2 Effect of stiffener height (*h*) on elastic wave propagation

According to Fig 3, there are also two obvious points 210kHz and 300kHz in the frequency domain of $R_{QQ'}$ and $\alpha_{QQ'}$ which divide the frequency domain into three regions. A conclusion similar to that of section 3.2 can be obtained. In addition, based on the second-order exponential form, $R_{QQ'}$ and $\alpha_{QQ'}$ can approximately fit three curves (I, II, III) in the range we discussed as shown in Fig 3, so that both of them can achieve extreme values under this relationship. In other words, under the working conditions involved, when *h* and *f* satisfy the relationship, the elastic wave propagates more easily through the stiffener, and the stiffener has little effect on the energy and phase of the elastic wave. At the same time, according to the calculation, the curve correlation coefficient is more than 0.9 under the condition of different stiffener thickness, that is, the influence of stiffener thickness parameters on the curve distribution can be ignored. Then the fitting equation can be written as follows:

$$h = a \cdot \exp(b \cdot f) + c \cdot \exp(e \cdot f) \tag{5}$$

The values of each coefficient of the curve are shown in Table 1:

Table 1. The value of each coefficient of the curve.

	I	II	III
a	9.30E+06	78.98	539.7
b	-0.5612	-0.01597	-0.02037
c	17.96	3.061	7.503
e	-0.0116	-8.61E-06	3.17E-04

4 Summary

In this paper, aiming at the spacecraft stiffener structure, combined with the finite element simulation and the measurement of laser Doppler vibrometer, its influence on elastic wave propagation is discussed and analyzed, and the relevant formulas are obtained. The conclusions of this paper are summarized as follows:

(1). The stiffener structure has a significant influence on the elastic wave propagation at different frequencies, and the influence degree is different. The elastic wave propagates through the stiffener mainly in two ways, one is through the wall, and the other is coupled to the stiffener. In the range of parameters involved in this paper, when the wavelength λ is greater than 10mm, the elastic waves propagate more easily through the wall, while most of them are reflected by the stiffener. When λ < 6mm, the elastic wave propagates are more easily through the stiffener, and the proportion increases.

(2). Compared with the thickness, the influence of the height of the stiffener on the propagation of elastic wave is more significant. Moreover, when the stiffener height and elastic wave frequency satisfy the second-order exponential relationship that proposed in this paper, the elastic wave propagates more easily by wall through the stiffener, and the influence of the stiffener on the elastic wave propagation is relatively small, which has almost nothing to do with the thickness of the stiffener.

This work was supported by the Science&Technology Development Fund of Tianjin Education Commission for Higher Education [grant numbers 2019KJ150].

References

1. Bian X, Li Y, Feng H, et al. A Location Method Using Sensor Arrays for Continuous Gas Leakage in Integrally Stiffened Plates Based on the Acoustic Characteristics of the Stiffener[J]. Sensors, **15**, 9:24644-24661 (2015)
2. Lhuillier P E, Chassignole B, Oudaa M, et al. Investigation of the ultrasonic attenuation in anisotropic weld materials with finite element modeling and grain-scale material description[J]. Ultrasonics, **78**: 40-50 (2017)
3. Pettit J R, Walker A E, Lowe M J S. Improved detection of rough defects for ultrasonic nondestructive evaluation inspections based on finite element modeling of elastic wave scattering[J]. IEEE Transactions on ultrasonics, ferroelectrics, and frequency control, **62**, 10: 1797-1808 (2015)
4. Shcherbinin S A, Shvetsov I A, et al. Finite element simulation of ultrasonic standing wave fields inside cylindrical piezoelectric transducers[J]. Ferroelectrics, **539**, 1:112-117 (2019)
5. Christensen, René. Modeling the Effects of Viscosity and Thermal Conduction on Acoustic Propagation in Rigid Tubes with Various Cross-Sectional Shapes[J]. Acta Acustica united with Acustica, **97**, 2:193-201 (2011)
6. Hongwei H , Zexiang W , Guangkai S , et al. Finite Element Simulation of Ultrasonic Guided Wave to Detect Through-type Defects in Pipe[J]. Journal of System Simulation, (2016)
7. AI Chun'an, HAN Zhaolin, LI Jian, et al. Research of Ultrasonic Simulation Based on FEM. Elementary Electroacoustics, **39**, 8: 39 (2015)
8. FU Xi Bin. COMSOL Simulation of Ultrasonic TOFD Detection of Pressure Vessel Welds. Nondestructive Testing, **40**, 007:9-14 (2018)
9. YE Hanfeng, TAO Meng, LI Junjie. Sound absorption performance analysis of anechoic coatings under oblique incidence condition based on COMSOL. JOURNAL OF VIBRATION AND SHOCK, **38**, 12: 213-218 (2019)